Geometric Inference of Building Boundaries by Fusing LiDAR Data Set with Aerial Photographs

Jen-Jer Jaw
Department of Civil Engineering, National Taiwan University
1 Roosevelt Rd. Sec. 4, Taipei,10617, Taiwan.
jejaw@ntu.edu.tw

Chieh-Chung Cheng
Department of Civil Engineering, National Taiwan University
1 Roosevelt Rd. Sec. 4, Taipei,10617, Taiwan.
r92521124@ntu.edu.tw

Abstract: The advent of LiDAR technique has opened up many possibilities for the purpose of object/surface reconstruction. The direct geo-referencing of 3-D laser point towards surface or terrain apparently outperforms photogrammetric method by employing at least two overlapping images in the data acquisition favor. It is, however, still inevitable to see some weaker characteristics of LiDAR system as compared to photogrammetric relatively high ground resolution and richer radiometric content revealed from the images. From the authors' point of view, LiDAR data set and aerial photographs are of complementary property whose evidence can be realized in reliable, yet less accurate LiDAR point cloud and precise, but ambiguous information in the photos. Therefore, fusion of above two data sets by utilizing mutual strengths for the purpose of reconstructing spatial information can be certainly optimistic and foreseen. In this study, the authors aim at extracting building boundaries by the following steps: (1). Hypothesizing 3-D building boundaries from LiDAR data set; (2). Back-projecting hypothesized 3-D building boundaries onto the associated photos; (3). Validation of building boundaries by imposing 2-D and 3-D geometric inferences in image space and in object space, respectively; (4). Merging and adjusting building boundaries. We conclude from this study that the proposed system offers more robust and satisfactory building reconstruction result as compared to the situation when only single data set is attempted.
Keywords: Geometric Inference, Back-projection, Fusion

1. Introduction

Line features, of higher-order information and easier detected than point features, are the main evidence for building hypotheses and reconstruction via photogrammetric approaches. Recently, the LiDAR systems have emerged as a new technology for rapidly capturing data on physical surfaces via active sensors for direct and reliable 3-D geometric information determination. Buildings, protruded above the ground, are apparent features and can be extracted with rough boundaries from LiDAR data set [1]. It has been reported and concluded that the LiDAR system is capable of offering a fast as well as effective way for acquiring building models in the urban site [2]. Fusing richer radiometric information offered by the photographs with reliable geometric information revealed from LiDAR data set for the purpose of building roof reconstruction would then gain better efficiency than employing only one source [3]. At current stage, due to the associated uncertainty, especially for the horizontal component, the roof boundaries provided from LiDAR data set are regarded as only approximations. 3-D building boundaries are determined by image line features geometrically inferring to this approximations. Namely, the approximation of building roof from LiDAR data set is refined and ultimately shaped after intersecting the most proper conjugate image line features upon imposing geometric inferences. In this study, the approaches as well as the strategies of geometric inference of building boundaries via the approximations from LiDAR data set have been proposed. Candidates of line features extracted from image pair are checked by 2-D and 3-D inferential rules that this study set and the building boundaries are finalized, leading to reconstructed roofs as the final product. The methods of geometrical inferences are in detailed elaboration in the next section.

2. Methodology

In this study, the rough building roofs, including flat (with or with parapets) and gable types, and 2-D line features in the images are regarded as input data. The main procedures designed for the proposed system are illustrated in Fig. 1. Due to the highly frequent occurrence of parapets for building roof of flat type, they are hypothesized in the inferential chain, seen also in Fig. 1(a).

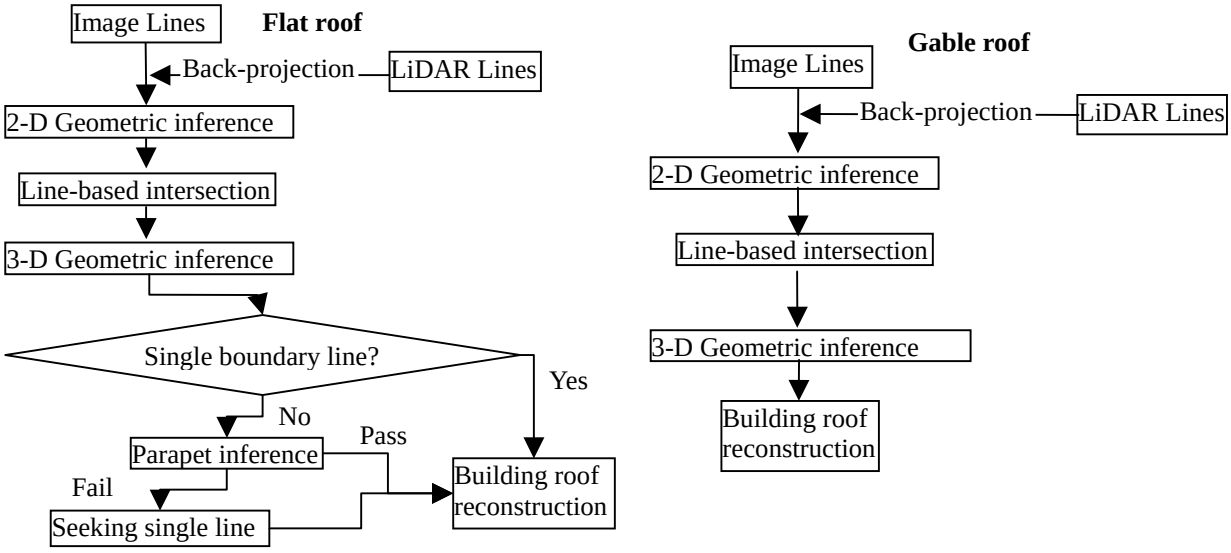

Fig. 1. Flowchart of geometric inference of building boundaries, flat type (a), gable type (b)

1) 2-D Geometric Inference for Flat Roofs

The boundaries of building roof from LiDAR data set are firstly back-projected onto the images. With the error budgets for LiDAR data set, orientation parameters and line feature measurement (or extraction) in the image, the size of buffer related to each projected LiDAR line feature can be formulated, thus inviting image line features that are present within this region. The buffers suitable for selecting the candidates can be estimated through "the law of error propagation".

1. Distance Check

The formula in Eq. (1) is used to calculate the distance of projected LiDAR line feature and those nearby image line features.

$$d = \frac{|ax + by + 1|}{\sqrt{a^2 + b^2}} \tag{1}$$

where (x, y): the coordinates of center of image line segment;

(a, b): the line parameters of projected LiDAR line;

The uncertainty of this distance can be estimated by taking the error sources into account using the law of error propagation. The threshold for distance check can be set as 2 to 3 times of standard deviation of the distance. Only those distances less than the threshold are survived and the associated line segments are regarded as candidates.

2 Angle Check

The angles between image line segments and projected LiDAR line is calculated by using Eq. (2). The angle threshold can be set with the similar approach as that for distance check. Again only those line segments with angles under the threshold are kept.

$$\cos\theta = \frac{\vec{AB} \bullet \vec{CD}}{|AB||CD|} \tag{2}$$

where $\vec{AB}, \vec{CD}$: the directional vector of projected LiDAR line and image line, respectively;

$|AB|, |CD|$: the length of $\vec{AB}, \vec{CD}$ segments;

3. Topology Check

The purpose of this inspection is to further filter out the image lines which although pass both the distance and angle checks but obviously are still too far away from projected LiDAR line segment. The topology of one feature to another can be notated by positive and negative symbols to present two opposite topological relationships. In Fig. 3, red lines

indicate the projected LiDAR line segments, while lines with other colors are the image lines. To check the closeness of candidate lines to the projected LiDAR line "A", the topologies of "A" to its neighbors "B" and "D" are determined via the spatial relationship of center of "A" segment to "B" and "D" line segments. Similarly, the individual topologies of all the candidate image line segments of "A" to "B" and "D" are established. Those candidate image line segments disapproving the projected LiDAR line segment will be excluded from the candidate list. The example in Fig. 3 shows that only the yellow image line segment remains as the candidate of "A" after applying topology check.

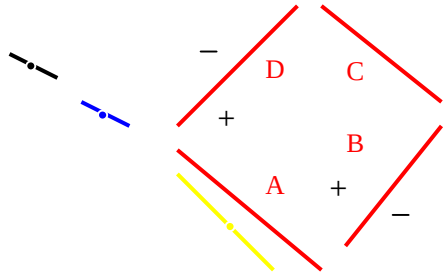

Fig. 3. Illustration of topology check

2) Line-based Intersection

Fig. 4 depicts the geometric representation of 3-D line intersection by conjugate 2-D line pair. The interpretation plane, passing through perspective center, image line, gives the solution space of 3-D line. The intersection of two conjugate interpretation planes determines the 3-D line in the object space. With this configuration, not only can the trajectory of 3-D line be mathematically traced, but also 3-D coordinates of the end points of the image line segment are able to be calculated.

Notations in Fig. 4:

O', O'': perspective centers in left and right images;

l', l'': line observation in left and right images;

$e' e''$: interpretation planes for two measured lines l', l'';

n_1, n_2: the normal vector of interpretation plane in the left and right image, respectively;

p_i: image coordinates of the end point of line segments;

P_i: object coordinates of the end point of line segments;

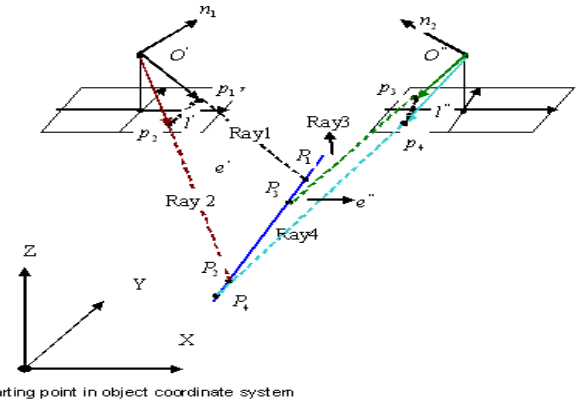

tarting point in object coordinate system

ıstration of line-based 3-D line determination

3) 3-D Geometric Inferences

Upon performing 2-D geometric inferences, the conjugate candidate image line segments for each building boundary are intersected into object space and the end points of 3-D line segment are obtained. Multiple 3-D line candidates would be expected and need to be further justified through the following inferential rules by employing angle and distance checks.

1. Angle and Distance Check in Object space

The check procedures are analogical to the ones in 2-D geometric inferences. The thresholds of distance and angle check in 3-D space are set according to the results estimated by applying the law of error propagation. The resulting 3-D lines that satisfy both distance and angle checks will be picked as building boundary candidates for roof reconstruction. Note that the multiple 3-D lines are to be observed due to the presences of parapets, if any. A statistic test would then serve to identify the presence of parapets.

2. Threshold for roof with Parapet

In general, the thickness of parapet seldom exceeds one meter on which basis the threshold of thickness of parapet can be assigned. Parapets can be hypothesized if met with multiple 3-D lines for sides of building roof and tested for

verifying the hypotheses.

3. Statistic Test of the Height of the Parapet

The top of parapets is assumed to be a horizontal plane for fulfilling most of the cases in reality. For this study, the authors utilize χ^2 distribution of statistic test to determine the most proper pair of candidate 3-D lines that correspond to the inner and outer sides of the parapets. The standard deviation used for this test can be acquired by manually selecting eight points located on the inner and outer sides of the parapet that are regarded as the model prototype. The statistic tests on all the candidates under a significance level (5% in this work) are then performed and the results that pass the tests are retained as the best solution for parapet determination.

4. Seeking the Best Solution among Multiple Lines

For the multiple candidate lines for a single boundary when failed to formulating parapet, the choice should be made as for which one to be picked as the best solution. With the assumed flat roof, the authors aim at height component and employ cost function, as illustrated in Eq. (3), for this purpose.

$$Cost(N_j, O) = \sum_{i=1}^{4} W_{ij} \left| L_{ij} - O \right| \qquad (3)$$

where:

L_{ij} : the height of four points on the L_j line; $i = 1..4; . j : the \quad j^{th}$ line candidate;

O : the height average of all confirmed boundaries;

W_{ij} : weight of the associated heights, assuming 1s in this case;

Each candidate line will be associated with one cost value according to Eq. (3). The best solution for the boundary can be found by taking the line with the minimum cost value.

4) Geometric Inference for Gable Roofs

The geometric inference methods used for flat roof are employed exactly for gable roof except that the roof is divided into left part and right part and processed separately before they are merged.

3. Experimental Results and Discussion

Four buildings with flat roofs (Fig. 5(a) and (b)) and one building with gable roof (Fig. 8(b) and (c)) were selected for demonstrating the feasibility of the proposed approaches. The test area is in Hsinchu, Taiwan. The LiDAR data sets was collected in 2002 by airborne laser scanning system while the images with scale of 1:5800, B/H=0.225, were taken almost the same time as the LiDAR data set.

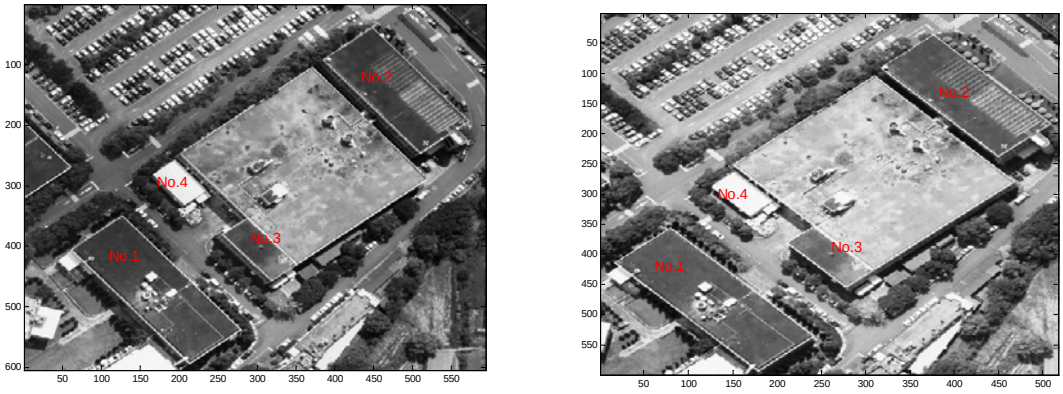

(a) (b)

Fig. 5. Four buildings for flat roof reconstruction, left image (a), right image (b)

1) Geometric Inference of Flat Roofs

The LiDAR point cloud and the extracted 3-D building roof are illustrated in Fig. 6 (a). Image lines in the left and right images are shown in Fig. 6 (b) and (c), respectively. Red lines in Fig. 6(d) and (e) represent the projected LiDAR line features. Through 2-D geometric inferences by distance, angle and topology checks, the candidates remain as indicated by blue lines in Fig. 6(d) and (e). The conjugate 2-D line segments then formulate 3-D line segments via

line-based intersection technique, as shown in Fig. 6(f). Note that there are multiple lines that are still present as candidates for each boundary at this stage. Fig. 6(g) gives the result upon 3-D geometric inference in object space, resulting in fewer 3-D line candidates as compared to that in Fig. 6(f). The multiple line candidates are then processed through parapet hypotheses and verification is concluded. The corresponding image lines that are selected for the building boundaries by the system are checked in Fig. 6(h) and (i) and the satisfactory result is manually justified.

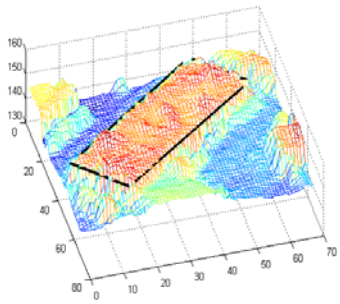

(a) Flat roof from LiDAR

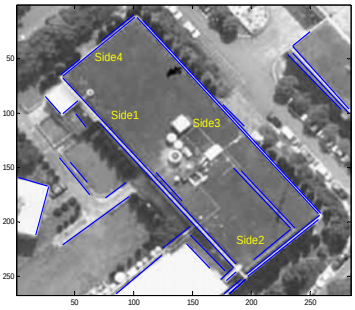

(b) Left Image lines

(c) Right image line

(d) LiDAR lines and left image lines

(e) LiDAR lines and right image lines

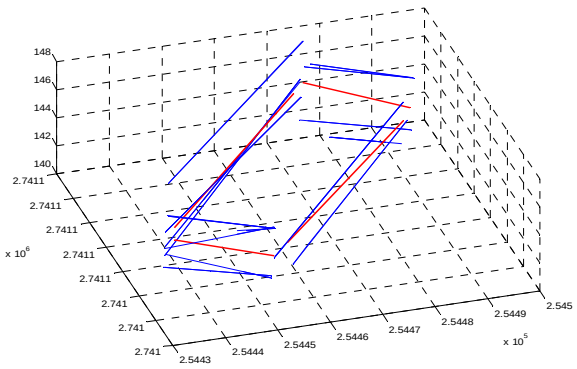

(f) Multiple 3-D lines upon 2-D geometric inference

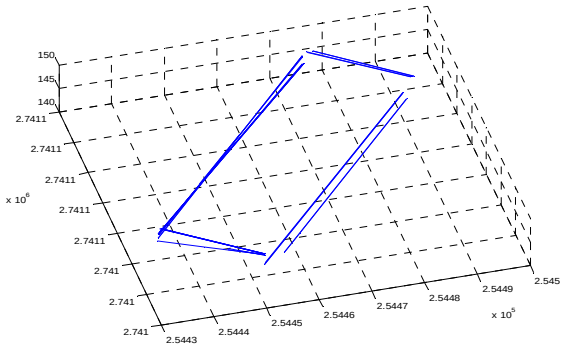

(g) 3-D lines upon 3-D geometric inference

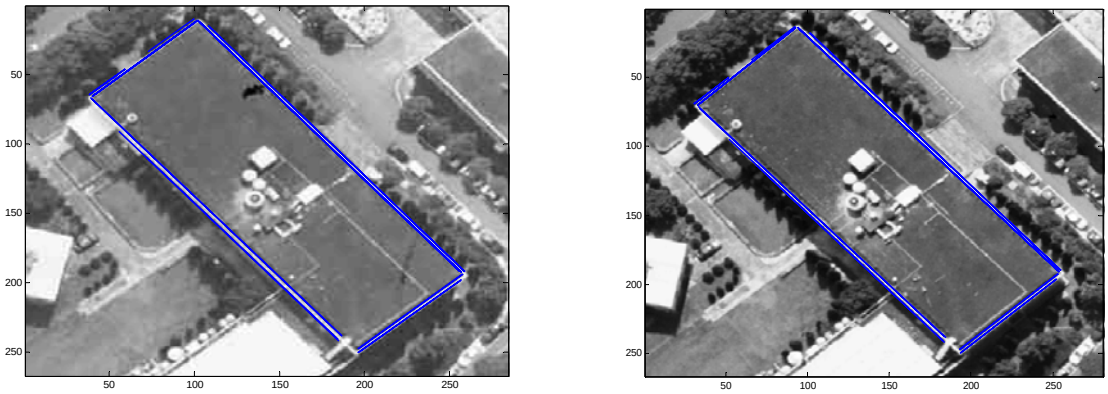

(h) The left image lines upon geometric inferences **(i) The left image lines upon geometric inferences**

Fig. 6. The intermediate results of geometric inferences of building no.1

The geometric inference procedures have been applied to all four buildings and the result of building roof reconstruction can be seen in Fig. 7.

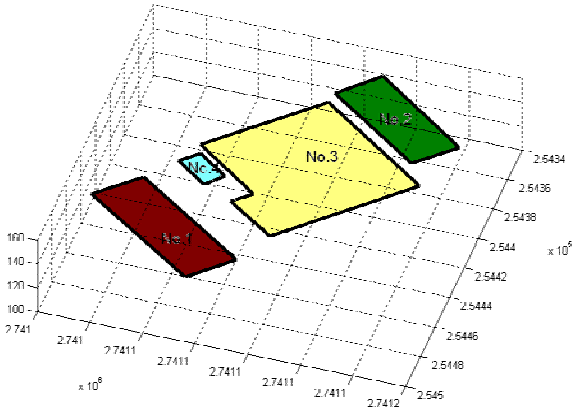

Fig. 7. The reconstruction result of four flat roofs

2) Geometric Inference of Gable Roof

Fig. 8 illustrates the intermediate result of building of gable type via geometric inferences. Left part and right part of the roof have been separately processed. The results of 3-D lines of roof are shown in Fig. 8(f) and 8(i). The complete roof structure is established after merging two parts of roofs and can be seen in Fig. 8(j).

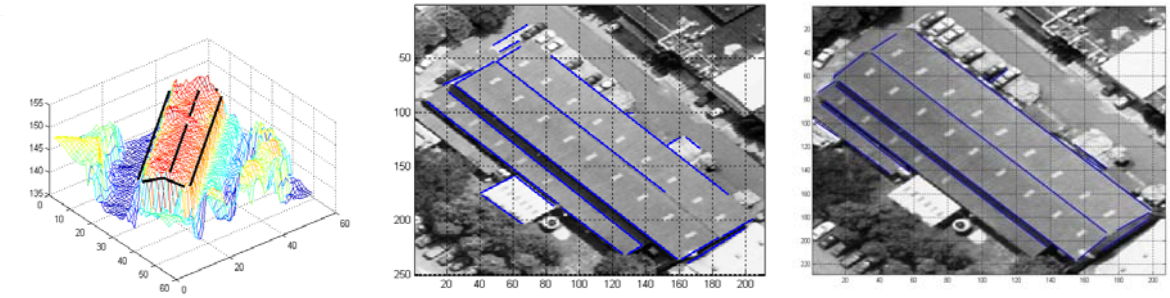

(a) Gable roof from LiDAR **(b) Left Image lines** **(c) Right image lines**

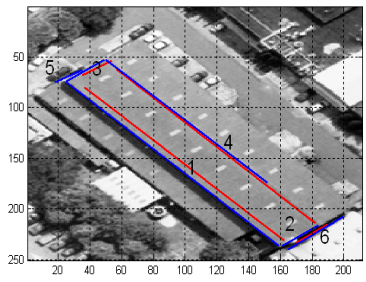

(d) LiDAR lines and left image lines for left part of the roof

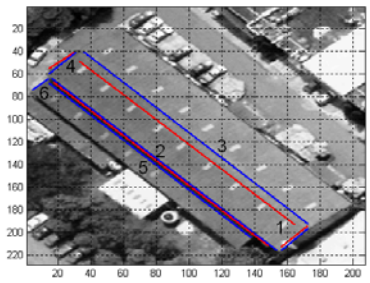

(e) LiDAR lines and right image lines for left part of the roof

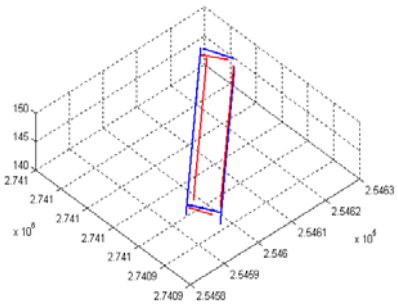

(f) 3-D lines of left part of the roof upon geometric inference

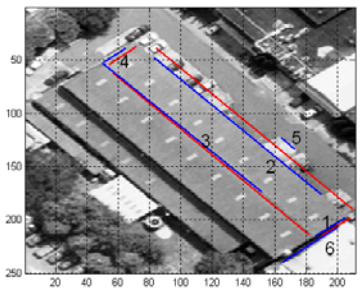

(f) LiDAR lines and left image lines for right part of the roof

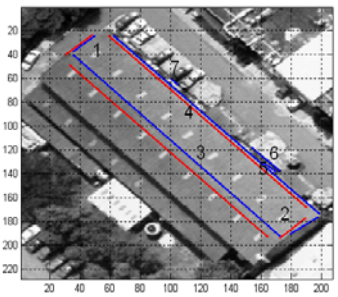

(g) LiDAR lines and right image lines for right part of the roof

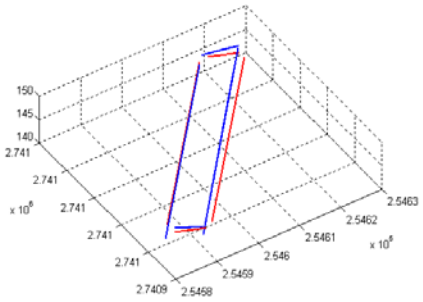

(f) 3-D lines of right part of the roof upon geometric inference

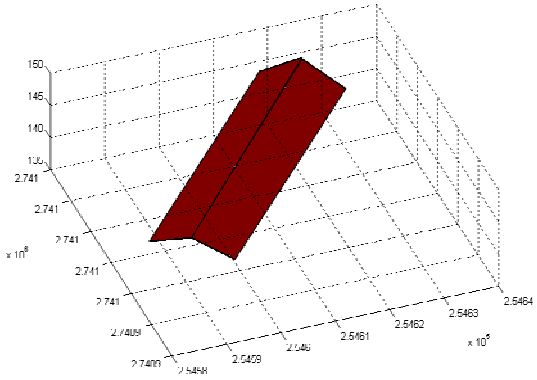

(j) Reconstruction result of gable-roof building

Fig. 8. The intermediate results of geometric inference of gable roof

4. Conclusions

The experimental results indicate that the proposed approaches by employing geometric inferences seem to be effective for reconstructing building roofs with flat and gable type. The addition of parapet hypotheses refines the solution when met with multiple line candidates.

Under current system design, the LiDAR data set is only treated as approximation, thus offering no metric contribution to the determination of building roof. As the research about the quality of airborne LiDAR data have reported its high accuracy potential for providing reliable geometric information, especially for the height component. Integrating LiDAR geometric information and making full use of influential component into the core of fusion process may promote the current result to a better quality both in accuracy and reliability levels.

Acknowledgement

The authors express their sincere gratefulness for National Science Council, Taiwan for partial support under the

grant of the project “NSC 93-2211-E-002-054”..

References

[1] Schenk, T., 2002. Fusion of LIDAR Data and Aerial Imagery for a More Complete Surface Description, IAPRS, vol. XXXIII, pp. 310-317.

[2] Ahmed, F.E. and S.B. James, 2002. Building Extraction Using LiDAR Data, *ASPRS-ACSM Annual Conference and FIG XXII Congress*.

[3] Rottensteiner, F., 2003. Automatic Generation Of Building Models From LIDAR Data and The Integration Of Aerial Images, ISPRS, Vol. XXXIV, pp.174-180.